Auger Resonant Raman Scattering in Itinerant Electron Systems: Continuum Excitation in Cu

A. Föhlisch,*,† O. Karis, M. Weinelt,‡ J. Hasselström, A. Nilsson, and N. Mårtensson

Department of Physics, Uppsala University, Box 530, S-751 21 Uppsala, Sweden

(Received 2 November 2000; published 28 December 2001)

The role of electron localization for resonant photoemission and Auger resonant Raman scattering to occur in an extended system was studied by polarization dependent resonant photoemission at the Cu L edges. Auger resonant Raman scattering was observed for continuum excitation into van Hove singularities at the $L_{(1)}$ and $X_{(1)}$ points, 4.2 and 7.7 eV above threshold. These findings show that resonant photoemission and Auger resonant Raman scattering are general features of photoemission independent of the degree of electron localization.

DOI: 10.1103/PhysRevLett.88.027601 PACS numbers: 79.60.Bm, 33.60.Fy, 71.27.+a

Resonant photoemission in the vicinity of a core-level threshold has become a powerful technique to study the electronic structure of matter in both fundamental research such as atomic and molecular science, and in the applied field of material science [1–11]. In particular for correlated materials—i.e., lanthanides, transition metals and their oxides—resonant photoemission has been a crucial tool for electronic structure investigations, i.e., the enhancement of the $4f$ and $5p$ component in rare earths and their com-pounds [5,7] or the Ni 6 eV photoemission satellite [8–10].

The basis of resonant photoemission is the opening of the Auger resonant Raman scattering channel at the core level threshold, which allows reaching the same final state via the interfering channels of Auger resonant Raman scattering and direct photoemission [1–4]. The interference has been successfully parametrized by the Fano resonance profile [12] and can be determined experimentally by polarization dependent measurements [10]. In Auger resonant Raman scattering, the absorption and decay processes must be considered as a single process (one step or coherent process) [3,13]. In contrast, normal Auger decay is commonly seen as a "two step" or incoherent process, where the emission of the Auger electron is independent from the initial absorption process, thus leading to emission at constant kinetic energy. Experimentally, scattering into a localized intermediate state is manifested through a linear dispersion of spectral features with photon energy and characteristic line narrowing below the natural linewidth of the core-hole intermediate state, conserving the bandwidth of the scattered radiation [3,4,13–15].

A controversial issue has been whether Auger resonant Raman scattering requires localized absorption resonances, and to what degree the occurrence of Auger resonant Raman scattering can be taken as an experimental measure of electron localization. For the simple metal potassium, autoionization of itinerant/delocalized intermediate states has been proposed to explain valence band photoemission features around the energetic shallow M edges [16]. Investigations of Auger resonant Raman scattering below and at core level thresholds have established the importance of unoccupied density of state effects in the shape of Auger resonant Raman spectral features as a general characteristic of Auger resonant Raman scattering [3,6,13,17]. However, the clear experimental proof of Auger resonant Raman scattering below threshold and for localized intermediate states could only support conjectures on the general occurrence of Auger resonant Raman scattering also for itinerant/delocalized intermediate states even above the ionization threshold [6,10,11].

In this Letter, we investigate the fundamental connection between the degree of electron localization in an extended system and the occurrence of coherent vs incoherent scattering. We studied Auger resonant Raman scattering at two polarizations to determine unambiguously the Auger resonant Raman channel in Cu which is one of the most studied materials by photoemission spectroscopy [18] with a well-resolved spectrum of the occupied $3d$ band. We find dominant Auger resonant Raman scattering for the $3d^8$ final states at the L_3 and L_2 edges and negligible direct photoemission. Surprisingly, we observe deviations from the constant kinetic energy of the Cu $L_3M_{4,5}M_{4,5}$ and $L_2M_{4,5}M_{4,5}$ normal Auger lines for continuum excitation 4.2 and 7.7 eV above the respective thresholds, not accounted for in the framework of Auger decay. These deviations at critical points at the L_1 and X_1 points in the fcc Cu first Brillouin zone are fully described by a simple energy conserving numerical model of Auger resonant Raman scattering, neglecting channel interference. The results show that Auger resonant Raman scattering can be supported to a significant fraction via delocalized/itinerant intermediate states, identifying resonant photoemission and Auger resonant Raman scattering as a general feature of photoemission, independent of the electron localization in a system.

The experiments were performed with a Scienta SES 200 [19] at BL 8.0 ALS of the Lawrence Berkeley National Laboratory with linear polarized undulator radiation at $\approx 7°$ grazing angle and 5×10^{-11} torr. The Cu crystal was cleaned by cycles of Ar^+-sputtering and annealing to 900 K, checked by LEED and XPS. In the Auger resonant Raman measurements with kinetic

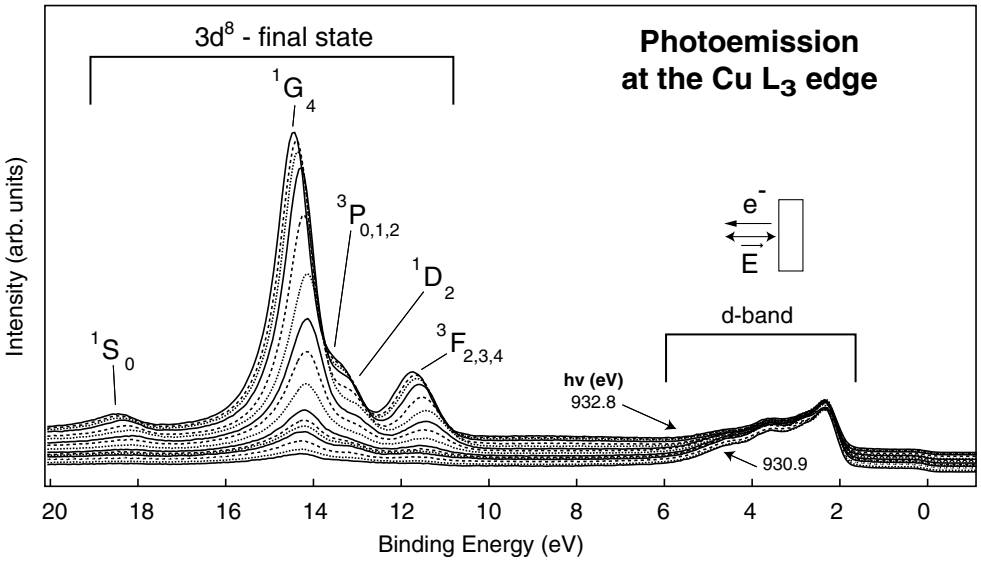

FIG. 1. Resonant photoemission on Cu(110) in the vicinity of the Cu L_3 edge at 932.8 eV.

energies exceeding 915 eV valence states across the first Brillouin zone are sampled. Each spectrum has been normalized to the photon flux on a gold grid.

Figure 1 contains photoemission spectra, measured at photon energies in the vicinity of the Cu L_3 edge at 932.8 eV in the photoemission geometry, where the electric field vector of the synchrotron radiation is parallel to the direction of electron detection. The spectra consist of the valence band photoemission from the Cu $4sp$ band between 0 and 1.8 eV and the Cu $3d$ band between 2 and 6 eV. The Cu $3d^8$ final states lie between 10 and 20 eV and can be reached by two channels: (i) Auger resonant Raman scattering, $2p^6[3d^{10}4s^1] \xrightarrow{V_r} 2p^5 3d^{10}[4s^2] \xrightarrow{V_A} 2p^6 3d^8[4s^2]$. (ii) Direct photoemission and ground state configuration interaction (CI), $2p^6[3d^{10}4s^1] \xrightarrow{\mathrm{CI}} 2p^6 3d^9[4s^2] \xrightarrow{V_r} 2p^6 3d^8[4s^2]$. Square brackets stand for electrons in delocalized states, including screening electrons, in contrast to localized atomiclike states, which are written without brackets. The photoemission features in the valence region are at constant binding energy for all photon energies, i.e., they have linear dispersion in kinetic energy. The $3d^8$ final states exhibit a rich multiplet structure, dominated by the $^1G_4$ final state [20], and show the well-known transformation from linear dispersion in kinetic energy below the core level threshold (L_3) to a constant kinetic energy feature above threshold, commonly attributed to Auger resonant Raman scattering below and at threshold and normal Auger behavior above threshold.

In Fig. 2 the photon energy dependence of the $3d^8\,{}^1G_4$ peak position (top panel) and intensity (middle panel) is summarized. Each point in Fig. 2 is extracted from a photoemission spectrum. Open circles represent a photoemission spectrum measured with the electric field vector of the synchrotron radiation parallel to the direction of detection (photoemission geometry) and full dots a spectrum measured with the electric field vector perpendicular to the direction of detection (auger geometry). The $3d^8\,{}^1G_4$ peak intensities and positions are very similar for the two geometries, indicating negligible direct photoemission. In particular, the $3d^8\,{}^1G_4$ intensities resemble the Fano resonance profile of a dominant Auger resonant Raman channel.

Let us now focus on the $3d^8\,{}^1G_4$ peak position in Fig. 2. Below the L_3 edge, linear dispersion with photon energy is found, as expected from Auger resonant Raman scattering. At threshold, the linear dispersion of the Auger resonant

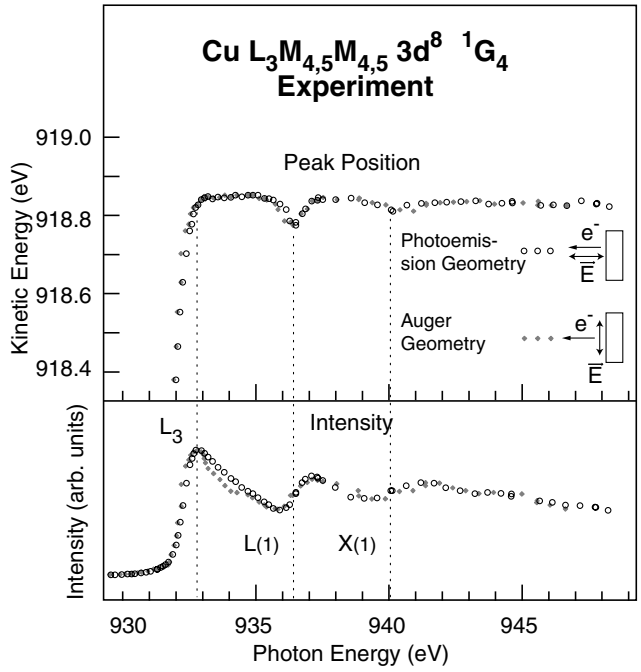

FIG. 2. Photon energy ($h\nu$) dependence of the $L_3M_{4,5}M_{4,5}$ $3d^8\,{}^1G_4$ final state. Comparison between measurements in the photoemission geometry (open circles) and the auger geometry (black dots). Top: $3d^8\,{}^1G_4$ peak position. Bottom: $3d^8\,{}^1G_4$ peak intensity.

Raman feature rather abruptly becomes the constant kinetic energy feature of the normal Auger decay up to 2 eV above threshold. However, at even higher photon energies significant deviations from constant kinetic energy to lower kinetic energies are found, coinciding with increasing absorption cross sections at 4.2 and 7.7 eV above the L_3 edge. In particular, the deviation at 4.2 eV above the L_3 edge is 0.07 ± 0.01 eV. This constitutes a significant deviation from the expected constant kinetic energy of normal Auger decay.

To assess the underlying mechanism of this behavior we calculated as a function of the photon energy $h\nu$ the lineprofile $I(\epsilon_A, h\nu)$ of the $3d^8\,{}^1G_4$ final state in a simple numerical simulation neglecting channel interference, which has been successfully used to describe Auger resonant Raman scattering in extended systems below threshold [6].

$$I(\epsilon_A, h\nu) = C \int_0^\infty \frac{\rho(\epsilon)\, d\epsilon}{[(h\nu - \epsilon - E_L)^2 + \Gamma_L^2/4][(h\nu - \epsilon - \epsilon_A - E_{M_4,M_5})^2 + \Gamma_{M_4,M_5}^2/4]}. \quad (1)$$

The dipole transitions from the L shell to the unoccupied d and s band are modeled by the weighted ground state partial sd-DOS $\rho(\epsilon)$ [21,22], neglecting core-hole relaxation [23]. The Auger matrix elements are given by the constant C. The lifetime broadening of the core-hole state at the energy E_L is $\Gamma_{L_3} = 0.41$ eV, in agreement with Refs. [24,25]. Furthermore, the lifetime broadening of the M_4, M_5 2-hole final state is taken from Refs. [26] as $\Gamma_{M_4,M_5} = 0.17$ eV at the energy E_{M_4,M_5}. In Fig. 3 the calculated peak intensity and position is shown with the theoretical sd-DOS used in the simulation. The experimental peak positions are in good agreement with the Auger resonant Raman calculation and the experimentally observed dips towards lower kinetic energy are reproduced in our numerical simulation and coincide with the $L_{(1)}-$ and $X_{(1)}-$van Hove singularities in the unoccupied band structure of Cu. The experimental deviation at the $L_{(1)}$ point is 0.07 ± 0.01 eV and the calculated value is 0.07 eV. Also the experimental and calculated $3d^8\,{}^1G_4$ peak intensities agree well except for some discrepancy at threshold, with larger experimental intensity than in the calculation. We interpret this additional intensity as the well-known many-body x-ray edge divergence [27] which is neglected in the one-electron simulation.

To test our interpretation of Auger resonant Raman scattering into itinerant continuum states further, we can now analyze the behavior above the Cu L_2 edge. Here the measurements took place under identical conditions in the photoemission geometry and the experimental $3d^8\,{}^1G_4$ peak position and intensity are shown in Fig. 4. As at the

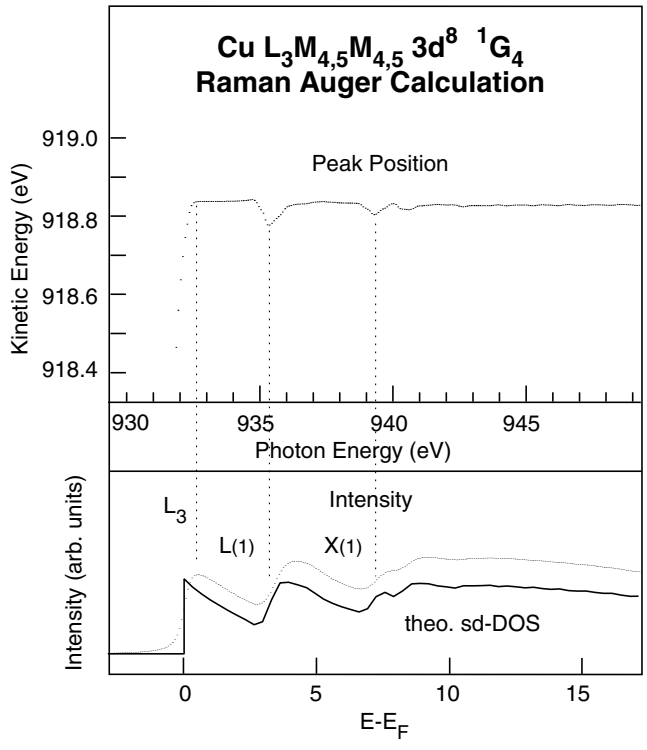

FIG. 3. Auger resonant Raman numerical model of the photon energy dependence of the $L_3M_{4,5}M_{4,5}$ $3d^8\,{}^1G_4$ final state. Top: $3d^8\,{}^1G_4$ peak position. Bottom: $3d^8\,{}^1G_4$ peak intensity and the theoretical sd-DOS used in the calculation.

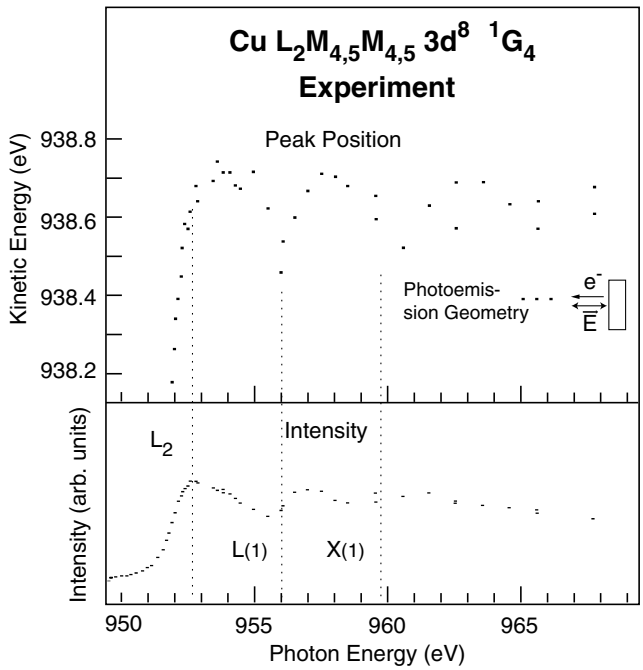

FIG. 4. Photon energy dependence of the $L_2M_{4,5}M_{4,5}$ $3d^8\,{}^1G_4$ final state in the photoemission geometry. Top: $3d^8\,{}^1G_4$ peak position. Bottom: $3d^8\,{}^1G_4$ peak intensity.

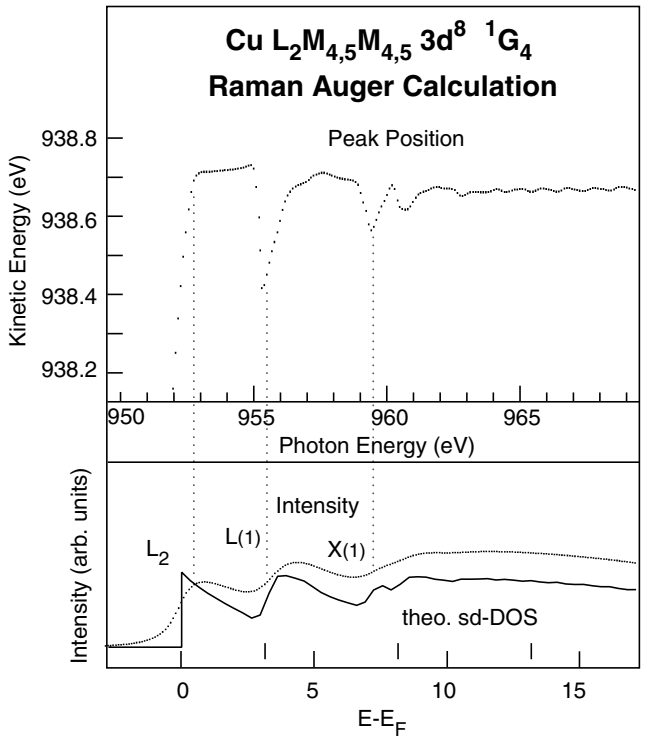

FIG. 5. Auger resonant Raman numerical model of the photon energy dependence of the $L_2M_{4,5}M_{4,5}$ $3d^8\,{}^1G_4$ final state. Top: $3d^8\,{}^1G_4$ peak position. Bottom: $3d^8\,{}^1G_4$ peak intensity and the theoretical *sd*-DOS used in the calculation.

L_3 edge, the $3d^8\,{}^1G_4$ peak exhibits significant deviations from constant kinetic energy to lower kinetic energy, at the $L_{(1)}-$ and $X_{(1)}-$van Hove singularities 4.2 and 7.7 eV above the L_2 edge. However, the deviation at the $L_{(1)}$ point is with 0.26 ± 0.04 eV much larger as above the L_3 edge with 0.07 ± 0.01 eV. We now performed the Auger resonant Raman calculation for the $3d^8\,{}^1G_4$ peak position and intensity at the L_2 edge with all parameters unchanged, except for the larger lifetime broadening, $\Gamma_{L_2} = 1.09$ eV [24,25], of the L_2 core hole due to the additional $L_3L_2M_{4,5}$ Coster-Kronig decay. This calculation is shown in Fig. 5. In good agreement to experiment, a deviation of 0.3 eV from constant kinetic energy at the $L_{(1)}$ point above the L_2 edge is found. These characteristic deviations from kinetic energy at the $L_{(1)}-$ and $X_{(1)}-$van Hove singularities above the L_2 and L_3 edges and their variation in magnitude in relation to the different L_2, L_3 core hole lifetimes unambiguously establish the occurrence of Auger resonant Raman scattering into these continuum states.

In conclusion, Auger resonant Raman scattering is found to occur to a large fraction via itinerant continuum states. This is manifested through deviations from the constant kinetic energy, expected for the normal auger decay for continuum excitation, at the $L_{(1)}$ and $X_{(1)}$ critical points of the Cu band structure. These findings give experimental support, that both for threshold and continuum excitation Auger resonant Raman scattering and resonant photoemission are general features of the photoemission process independent of the degree of electron localization in a system.

We thank M. Magnuson for stimulating discussion. This work was supported by the Swedish Natural Science Research Council (NFR) and the Göran Gustavsson Foundation for Research in Natural Sciences and Medicine.

*Corresponding author.
Electronic address: alexander.foehlisch@desy.de
†Present address: Institut für Experimentalphysik, Universität Hamburg, Luruper Chaussee 149, D-22761 Hamburg, Germany.
‡Present address: Lehrstuhl für Festkörperphysik, Universität Erlangen-Nürnberg, Staudtstrasse 7, A3, D-91058 Erlangen, Germany.

[1] *Narrow-Band Phenomena: Influence of Electrons with both Band and Localized Character,* edited by J. C. Fuggle, G. Sawatzky, and J. Allen (Plenum Press, New York, 1988).
[2] C.-O. Almbladh and L. Hedin, in *Handbook on Synchrotron Radiation,* edited by E.-E. Koch (North-Holland Publishing Company, Amsterdam, 1992), Vol. 1B.
[3] T. Åberg and B. Craseman, in *Resonant Anomalous X-ray Scattering,* edited by G. Materlik, C. Sparks, and K. Fischer (North-Holland, Amsterdam, 1994).
[4] F. Gel'mukhanov and H. Ågren, Phys. Rep. **312**, 87 (1999).
[5] J. W. Allen *et al.,* Phys. Rev. Lett. **46**, 1100 (1981).
[6] W. Drube, R. Treusch, and G. Materlik, Phys. Rev. Lett. **74**, 42 (1995).
[7] S. R. Mishra *et al.,* Phys. Rev. Lett. **81**, 1306 (1998).
[8] C. Guillot *et al.,* Phys. Rev. Lett. **39**, 1632 (1977).
[9] S. Hüfner and G. K. Wertheim, Phys. Lett. A **51**, 299 (1975); **51**, 301 (1975).
[10] M. Weinelt *et al.,* Phys. Rev. Lett. **78**, 967 (1997).
[11] L. H. Tjeng *et al.,* Phys. Rev. B **48**, 13 378 (1993).
[12] U. Fano, Phys. Rev. Lett. **124**, 1866 (1961).
[13] T. Åberg, Phys. Scr. **T41**, 3271 (1992).
[14] A. Kivimäki *et al.,* Phys. Rev. Lett. **71**, 4307 (1993).
[15] S. Aksela *et al.,* Phys. Rev. Lett. **74**, 2917 (1995).
[16] G. K. Wertheim and D. M. Riffe, Solid State Commun. **96**, 645 (1995).
[17] J. C. Fuggle and G. A. Sawatzky, Phys. Rev. Lett. **66**, 966 (1991).
[18] R. Courths and S. Hüfner, Phys. Rep. **112**, 55 (1984).
[19] N. Mårtensson *et al.,* J. Electron Spectrosc. Relat. Phenom. **70**, 117 (1994).
[20] E. D. Roberts, P. Weightman, and C. E. Johnson, J. Phys. C **8**, L301 (1979).
[21] A. Niklasson, O. Eriksson, and B. Johansson, (unpublished).
[22] H. Skriver and N. Rosengaard, Phys. Rev. B **43**, 9538 (1991).
[23] H. Ebert *et al.,* Phys. Rev. B **53**, 16 067 (1996).
[24] A. Lebugle *et al.,* Phys. Scr. **23**, 825 (1981).
[25] J. C. Fuggle and J. E. Inglesfield, in *Topics in Applied Physics,* edited by J. C. Fuggle and J. E. Inglesfield (Springer, Berlin, 1992), Vol. 69.
[26] H. Petek, H. Nagano, and S. Ogawa, Phys. Rev. Lett. **83**, 832 (1999).
[27] L. Davis and L. Feldkamp, Phys. Rev. B **23**, 6239 (1981).